RSC Advances

ROYAL SOCIETY
OF CHEMISTRY

www.rsc.org/advances

RSC Advances

Dynamic Article Links ▶

COMMUNICATION

BiOBr Photocatalyzed Decarboxylation of Glutamic Acid: Reaction Rates, Intermediates and Mechanism

Yanfen Fang,[a,b] Hongwei Yang,[a,b] Wei Zhou,[a,b] Yue Li,[c] David M. Johnson,[a,b] and Yingping Huang*[a,b]

The degradation of glutamic acid by BiOBr under both UV and visible irradiation were investigated and compared with degradation by TiO_2/UV. Analysis of reaction rates and the distribution of intermediates was used to show that both BiOBr 10 systems, unlike the TiO_2 system, catalyze direct substrate oxidation by valance band holes.

Visible light photocatalysis has attracted continuing attention because of potential applications in water purification.[1,2] A recently developed photocatalyst, BiOBr, is an efficient visible 15 light photocatalyst [3-5] with visible light activity higher than that of N-doped TiO_2.[6] As described previously, BiOBr has two discreet valance bands produced from O-2p and Br-4p orbitals.[7-8] The two bands respond, respectively, to UV and visible light excitation and holes of different oxidation potential are generated, providing 20 multiple mechanisms for photocatalytic degradation.[7]

Amino acids are biologically important organic compounds, both as building blocks for proteins and as metabolic intermediates. As biodecomposition products, amino acids are distributed widely in natural waters.[9,10] The concentration of 25 amino acids in surface water is generally in the range of 2.5−60 nM.[11,12] Although amino acids are nontoxic, they can form carcinogenic and mutagenic species during the water purification process.[13,14] For example, amino acids were converted primarily to halomethanes and haloacetic acids by chlorination.[15-17] More 30 importantly, with naturally occurring toxins it is usually the carboxyl group of an amino acid that binds to the affected enzyme.[18-21] For example, with the well-known cyanotoxin, microcystin-LR, the free carboxyl groups on D-Glu and D-MeAsp bind with the metal atom and Arg96 of protein 35 phosphatase 1 (PP1) to inhibit protein phosphorylation.[19,20] Thus, understanding the degradation mechanism of amino acids, particularly the decarboxylation process, is of practical significance for water purification.

Glutamic acid (Glu) is one of the proteinogenic amino acids 40 and, with a second carboxyl group on the side chain, it is an ideal substrate for comparing the degradation process of carboxylic acids with that of amino acids. In this work, we used BiOBr as the photocatalyst to degrade Glu under both UV and Vis irradiation. The degradation process was examined with ^{1}H NMR 45 and ^{18}O isotope labeling and spin trapping ESR were used to elucidate the reaction mechanism. These results were compared with those from a TiO_2 system to show the effect of the valance band structure of BiOBr on the catalytic degradation of amino acids.

50 D_2O suspensions containing BiOBr and Glu were irradiated with UV or visible light for a given time and then analyzed using ^{1}H NMR analysis after removing the photocatalyst. Compared with parent substrate (Glu), the reacted solutions gave additional peaks at δ of 1.93, 2.48, 3.26 and 8.35 with both UV and visible 55 light irradiated systems (Fig. 1). Using reference compounds, these peaks were assigned to acetic acid (AA), succinic acid (SA), malonic acid (MA) and formic acid (FA). The change in the ^{1}H NMR spectrum with reaction time also provides the kinetics of substrate consumption and intermediate formation in 60 the BiOBr/UV and BiOBr/Vis systems (Fig. 2).
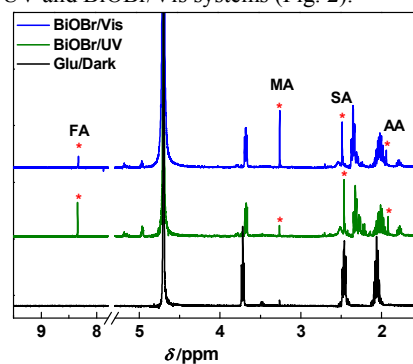
Fig. 1 ^{1}H NHR spectra of oxidative products of Glu in BiOBr/Vis and BiOBr/UV systems, 1 g L^{-1} BiOBr, c_{Glu}^0 = 10 mmol L^{-1}, 10 mL D_2O.

65
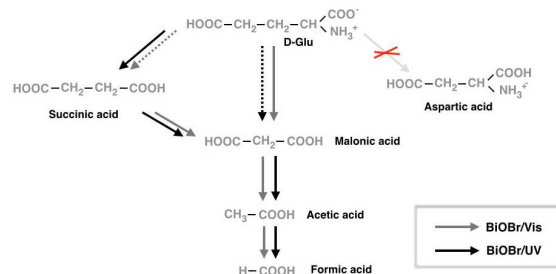
Scheme 1. Difference in the decarboxylation of Glu in BiOBr/Vis (gray arrows) and BiOBr/UV (black arrows) systems. Solid arrows shows a major reaction route, dashed arrows represent a minor reaction route.
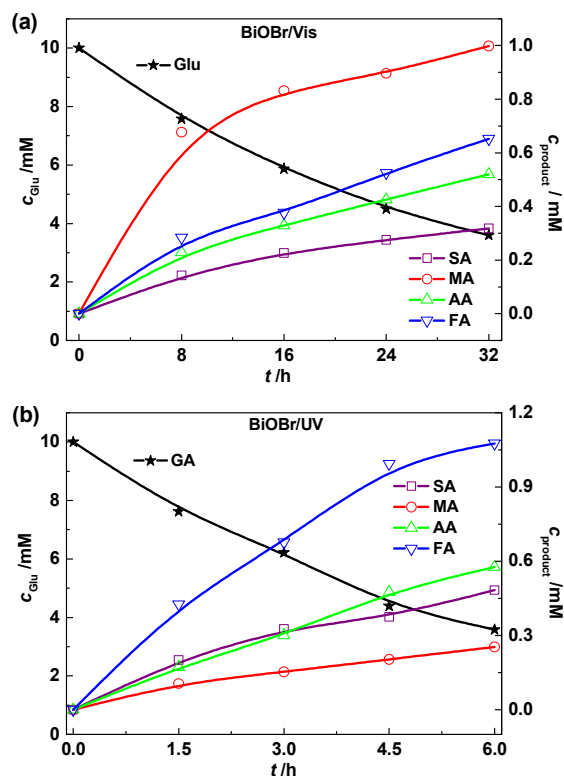
Fig. 2 Concentration change of substrate and oxidation products during photocatalytic oxidation of Glu in (a) BiOBr/ Vis system
5 and (b) BiOBr/UV system.

During photocatalytic oxidation, Glu forms SA initially and further reaction of the primary intermediate gives MA, AA and FA. However, no signal for aspartic acid, the decarboxylation
10 product of Glu, was recorded, a clear indication that degradation begins with the amino group rather than the carboxyl. The different decarboxylation of Glu in BiOBr/Vis and BiOBr/UV systems was proposed in Scheme 1 (additional details are shown in Fig. S1 (ESI†)). Similarly, during the BiOBr photocatalyzed
15 oxidation of microcystin-LR,[22] degradation also begins with oxidation of the amino-carboxyl structure of Glu. These results indicate that the amino-carboxyl structure is susceptible to oxidation in BiOBr photocatalytic systems. Due to the reactivity of this structure, amino acids are more readily degraded by
20 BiOBr than are free carboxylic acids.

Table 1. The formation rate and selectivity of intermediates produced in the photocatalytic degradation of Glu.

System	$r_d{}^a$ (mmol L^{-1} h^{-1})	$r_f{}^b$ (mmol L^{-1} h^{-1})		Sel. ^{c} (%)	
		SA	MA	SA	MA
BiOBr/Vis	0.199	0.019	0.055	9.6	27.8
BiOBr/UV	1.071	0.152	0.081	14.2	7.6
TiO₂/UV	13.33	0.197	0.173	1.5	1.3

^{a}Decomposition rate of Glu; ^{b}Formation rate of intermediate;
25 ^{c}Ratio of consumption rate of substrate to accumulation rate of intermediate.

The BiOBr/Vis and BiOBr/UV systems display different degradation kinetics, but the visible light irradiated system also shows lower selectivity for SA and a markedly higher selectivity for MA (Table 1). This phenomenon is attributed to the discrete
30 valance band structure of BiOBr. The holes generated by UV ($h_{O-2p}{}^+$) and visible light ($h_{Br-4p}{}^+$) excitation have different oxidation potentials, leading to different secondary reactions and the observed differences in rate. The results obtained in these systems were also compared with those of the classic TiO₂/UV system to
35 show the unique properties of BiOBr photocatalysis. It was observed that the TiO₂/UV photocatalyzed oxidation of Glu gave remarkably low intermediate concentrations. The total selectivity of SA and MA in the TiO₂ photocatalyzed system is only 2.8%, which is much lower than that of BiOBr/Vis and BiOBr/UV
40 systems (37.4% and 21.8%, respectively, Table 1). TiO₂ has a valance band ($E_{vb} = 2.7$ V) more oxidizing than either of the two valance bands of BiOBr and its hole oxidizes H₂O to ˙OH. It was reported that ˙OH plays a significant role in TiO₂ photocatalyzed degradation of amino acids.[23-25] Considering the valance band
45 potentials and differences observed between the BiOBr and TiO₂ systems, we assume that the valance band hole of both BiOBr systems initiates the degradation of Glu by direct oxidation rather than by ˙OH mediated reactions.

Table 2. Average isotope abundances of oxygen atoms in the
50 carboxyl group of SA in $H_2{}^{18}O$ isotope labeling experiments ^{a}

System	Time (min)	Substrate conv. (%)	SA yield (%)	Abundance^b (%)	
				$^{16}O_2$	$H_2{}^{18}O$
BiOBr/Vis	480	29.9	11.9	14.2	85.8
BiOBr/UV	90	23.8	23.8	13.1	86.9
TiO₂/UV	20	20.8	20.8	6.4	93.6

^{a}1 g L^{-1} photocatalyst, $c_{Glu}{}^0 = 10$ mmol L^{-1}, 2 mL $H_2{}^{18}O$; ^{b}Average value of the two O atoms of the formed carboxyl group, corrected with the oxygen isotope abundance of solvent $H_2{}^{18}O$ and the natural isotope abundance of aerial O₂.

55 Since the photocatalytic degradation of Glu starts from the amino-carboxyl end and leads initially to SA, the decarboxylated and deaminated product, we anticipated that the source of oxygen atoms in the carboxyl group formed in this process could give useful information about the mechanism of the reaction. These
60 experiments were carried out in ¹⁸O-enriched water ($H_2{}^{18}O$) and atmospheric ¹⁶O₂. Samples from the three systems were collected at times that resulted in similar substrate conversion (20−30%), and analyzed by derivative GC-MS (Fig. S2−S4(ESI†)). As shown in Table 2, O atoms from both H₂O and O₂ were
65 incorporated into SA under BiOBr photocatalysis condition. The SA formed in BiOBr/UV and BiOBr/Vis systems have similar isotope abundances of carboxyl O atoms (¹⁶O% = 13-14), which illustrates that these two systems react with similar mechanisms. In contrast, the SA formed in the TiO₂/UV system gave an ¹⁶O
70 abundance (¹⁶O% = 6.4) less than half that of the BiOBr systems. TiO₂ photocatalysis clearly incorporates more H₂O derived oxygen to the product than the BiOBr systems. We also performed ¹⁸O₂ isotope labeling experiments and similar results were obtained (Table S1 and Figures S5−S7 (ESI†)). Since the
75 valance band hole of TiO₂ can oxidize H₂O to ˙OH and incorporate O atoms from H₂O to the product, the higher proportion of H₂O derived oxygen in the TiO₂/UV system is reasonable. These results also corroborate the direct oxidation

mechanism proposed for BiOBr systems. We propose that, in both the BiOBr/UV and BiOBr/Vis systems, the photogenerated hole (h_{O-2p}^{+} or h_{Br-4p}^{+}) oxidizes Glu to a cation radical, which then reacts with either O_2 or H_2O to produce the carboxyl group on the product.

To further confirm that direct oxidation of Glu accounts for the larger pool of intermediates and higher proportion of O_2-derived oxygen in SA observed in the BiOBr systems, spin-trapping ESR spectroscopy was used to detect the formation of $\cdot$OH. The results were again compared with those of TiO_2 and are shown in Fig. 3. In contrast to the TiO_2/UV system, the signals from trapped $\cdot$OH recorded in the BiOBr systems was either weaker or nonexistent. Because neither of the valance band holes of BiOBr can oxidize H_2O, the small amount of $\cdot$OH is attributed to the reduction of O_2 by conduction band electrons ($O_2 \rightarrow \cdot OOH \rightarrow H_2O_2 \rightarrow \cdot OH$) and $\cdot$OOH was detected (Figure S8 (ESI†)).
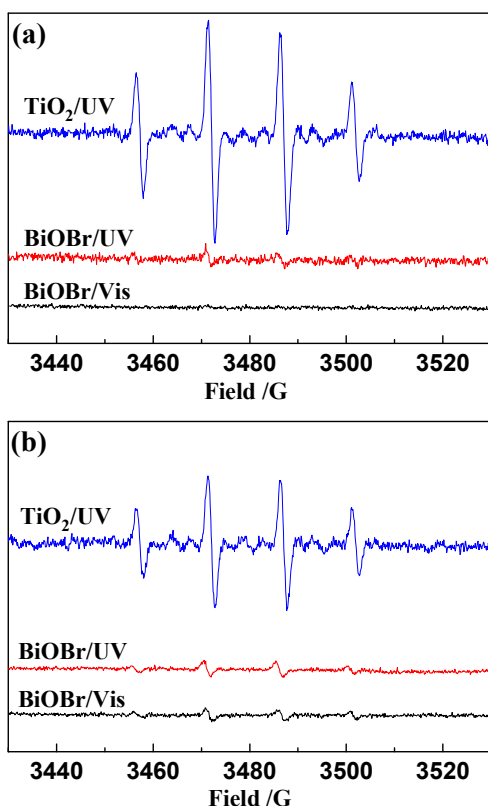

Fig. 3 ESR signals of the DMPO-$\cdot$OH adducts in TiO_2/UV, BiOBr/UV and BiOBr/Vis systems (a) without and (b) with Glu (10 mmol L^{-1}). 1 g L^{-1} photocatalyst, c_{DMPO} = 0.4 mol L^{-1}.

Conclusions

In summary, we studied the BiOBr catalyzed degradation of Glu under UV and visible light irradiation. Results indicate that, in both BiOBr/UV and BiOBr/Vis systems, the degradation process is initiated by direct substrate oxidation by the valance band hole. This, in turn, leads to the same primary product with the same source of oxygen in the carboxyl group formed on SA. However, the difference in the hole oxidation potentials of BiOBr/UV and BiOBr/Vis leads to different degradation rates, different secondary degradation processes and different distributions of degradation intermediates.

Notes and references

^{a} Innovation Center for Geo-Hazards and Eco-Environment in Three Gorges Area, Hubei province, Yichang 443002, China

^{b} Engineering Research Center of Eco-environment in Three Gorges Reservoir Region, Ministry of Education, China Three Gorges University, Yichang, 443002

^{c} Department of Chemistry, Nankai University, Tianjin 300071 (P.R. China)

* Corresponding author. Tel.: +86 717 6397488   Fax: +86 717 6395966. E-mail: huangyp@ctgu.edu.cn

† Electronic Supplementary Information (ESI) available: Experimental details, additional figures and tables. See DOI: 10.1039/b000000x/

1   R. Asahi, T. Morikawa, T. Ohwaki, K. Aoki and Y. Taga, *Science*, 2001, **293**, 269.
2   Z. Zou, J. Ye, K. Sayama and H. Arakawa, *Nature*, 2001, **414**, 625.
3   J. Li, Y. Yu and L. Zhang, *Nanoscale*, 2014, **6**, 8473.
4   H.F. Cheng, B.B. Huang and Y. Dai, *Nanoscale*, 2014, **6**, 2009.
5   S.L. Wang, W.H. Ma, Y.F. Fang, M.K. Jia and Y.P. Huang, *Appl. Catal. B Environ.*, 2014, **150-151**, 380.
6   J. Wang, Y. Zhang, L.Tian, F. Liu, Q. Xia, *J. Nanopart. Res.*, 2014, **16**, 2691.
7   Y.F. Fang, W.H. Ma, Y.P. Huang and G.W. Cheng, *Chem. Eur. J.*, 2013, **19**, 3224.
8   S.L. Wang, L.L. Wang, W.H, Ma, D.M. Johnson, Y.F. Fang, M.K. Jia and Y.P. Huang, *Chem. Eng. J.*, 2015, **259**, 410.
9   G. Absalan, M. Akhond and L. Sheikhian, *Amino Acids*, 2010, **39**, 167.
10   J.T. Edward, P. G. Farrell and J. L. Job, *J. Am. Chem. Soc.*, 1974, **96**, 902.
11   K. Tada, M. Tada and Y. Maita, *J. Oceanogr.*, 1998, **54**, 313.
12   N.O.G. Jørgensen and Limnol, *J. Oceanogr.*, 1987, **32**, 97.
13   C. Goeschen, N. Wibowo and J.M. White, *Org. Biomol. Chem.*, 2011, **9**, 3380.
14   D.P. Li, C.Y. Hu, Y.L. Lin and S.J. Xia, *Sci. Total. Environ.*, 2011, **409**, 1116.
15   T. Bond, J. Huang, M. R. Templeton and N. Graham, *Water. Res.*, 2011, **45**, 4321.
16   H.C. Hong, M.H. Wong and Y. Liang, *Arch. Environ. Con. Tox.*, 2009, **56**, 638.
17   T. Bond, N. H. M. Kamal and T. Bonnisseau, *J. Hazard. Mater.*, 2014, **278**, 288.
18   K.J. Ullrich, G. Rumrich, Th. Wieland and W. Dekant, *Pflug. Arch. Eur. J. Phy.*, 1989, **415**, 342.
19   A. Campos and V. Vasconcelos. *Int. J. Mol. Sci.*, 2010, **11**, 268-287.
20   C. Drahl, B. F. Cravattn and E.J, Sorensen. *Angew. Chem. Int. Ed.*, 2005, **44**, 5788.
21   A. Moshnikova, V. Moshnikova, O.A. Andreev and Y.K. Reshetnyak. *Biochemistry-US*, 2013, **52**, 1171.
22   Y. F. Fang, Y. P. Huang, J. Yang, P. Wang and G. W. Cheng, *Environ. Sci. Technol.*, 2011, **45**, 1593.
23   S. Horikoshi, N. Serpone, J. Zhao and H. Hidaka, *J. Photochem. Photobiol.*, A 1998, **118**, 123.
24   L. Elsellami, F. Vocanson, F. Dappozze, R. Baudot, G. Febvay, M. Rey, A. Houas and C. Guillard, *Appl. Catal. B Environ.*, 2010, **94**, 192.
25   M. Matsushita, T.H. Tran, A.Y. Nosaka and Y. Nosaka. *Catal. Today*, 2007, **120**, 240.